

Development of gold particles at varying precursor concentration

Mubarak Ali ^{a, *} and I –Nan Lin ^b

^a Department of Physics, COMSATS University Islamabad, Park Road, Islamabad-45550, Pakistan, *E-mail: mubarak74@comsats.edu.pk, mubarak74@mail.com

^b Department of Physics, Tamkang University, Tamsui, New Taipei City 25137, Taiwan

Abstract –Coalescence of tiny-sized particles into a large-sized particle has been an overlooked phenomenon since long. Present study discloses developing tiny-sized particles and their coalescence into large-sized particles under varying concentration of gold precursor in locally built setup namely, pulse-based electronphoton-solution interface process. Under the fixed ratio of pulse OFF to ON time, tiny-sized particles in different sizes develop depending on the amount of gold precursor. Packets of nano shape energy bind gold atoms into tiny-sized particles depending on the scheme of monolayer assembly at solution surface. Between precursor concentration 0.07 mM to 0.90 mM, many tiny-sized particles are developed in joined triangular-shape, they are in the large number at 0.30 mM and at 0.60 mM. On separation of joined triangular-shaped tiny particles into two under the exerting force along opposite poles of just connected atoms, each has the shape of an equilateral triangular-shape. Their atoms of one-dimensional arrays elongate under the exerting force of opposite poles converting into structures of smooth elements. Such tiny-sized particles pack to assemble structures of smooth elements where they terminate the exerting forces of surface format at central point of light glow resulting into develop geometric anisotropic particles. At 0.05 mM and 1.20 mM, to a large extent, tiny-sized particles do not develop in a triangular-shape where their packings deal mixed behavior of exerting forces for them resulting into develop distorted particles. Photons reflected at the surface of geometric anisotropic particles validate the order of structural regularity, which is not the case of distorted particles. Under different argon flow rate, morphology and structure of

particles alter to some extent. This study clarifies under what concentration of gold, a certain sized and shaped particle is developed.

Keywords: Precursor concentration; Nano shape energy; Tiny-shaped particles; One-dimensional particles; Multi-dimensional particles; Distorted particles

Introduction:

Developing the different structures of colloidal matter under certain processing strategy may be the origin of persuaded phenomenon where their controlled shape particles can be considered the strong candidates as high anisotropy of particles is remained a great challenge and under hot debate since decades. To assemble tiny-sized particles precisely is a goal for developing advanced functional materials. Metallic colloids having different shapes under varying concentration of precursor may indicate unexplored factors responsible for their development. When tiny-sized particle is developed under atom-to-atom amalgamation, attained dynamics of atoms are to be one of the causes. To regulate the structure of tiny-sized particles acquiring certain geometry following by developing structure of their large-sized particle, a tailored amount of shaped energy is to be another cause. Nature of the electron-dynamics of atoms regulating the structure and morphology to synthesize certain material can be the core cause as attained dynamics of atoms and tailored amount of shaped energy are not the only causes. It is expected that under varying the concentration of gold precursor, in an appropriate range, it may result into depict the overall picture of size, shape and structure of particles in different scales.

Several approaches have been enlisted in the literature to synthesize colloidal tiny-sized particles and large-sized particles where citrate reduction method is one of the most widely adopted procedures [1]. Development of large-sized particles on likely coalescence of tiny-sized particles has been the subject of several studies [2-12]. Metal clusters behave like simple chemical compounds and could find several applications in catalysis, sensors and molecular electronics [2]. Discrete features of nanocrystals and their tendency to extend into superlattices suggest ways and means for the design and fabrication of advanced materials with controlled characteristics [3]. An ordered array of nanoparticles instead of agglomeration might present new properties different from the

individual particles [4]. Coalescence of nanocrystals into extended shapes has been appeared to be a realistic goal [5]. Self-assembly means to design specific structure, which cannot be achieved alternatively [6]. Potential long-term use of nanoparticle technology is to develop small electronic devices [7]. Assembling of nanoparticles may be an initial effort towards the selective positioning and patterning at large area [8]. Organization of nanometer size building blocks into specific structures to construct functional materials and devices is one of the current challenges [9]. On assembling nanocrystals into useful structures 'atoms and molecules' will be treated as materials of tomorrow [10]. Precise control on the assemblies of nanoparticles enables the synthesis of complex shapes and will provide pathways to fabricate new materials and devices [11]. Coalescing nanocrystals into long-range crystals allow one to develop materials with endless selections [12]. Anisotropic shapes have the size-dependent surface plasmon absorption, but it remained challenging to take benefit of the phenomenon at macroscopic level [13].

On trapping mobile electrons, tiny particles of gold collectively oscillate [14]. The existing mechanistic interpretations are insufficient to explain several observations and rate of reactant addition/reduction can be estimated to produce subsequent specific shaped particles in high yields [15]. Locating the specific mode of excitation of surface plasmon in metallic nanocrystals will bring intense consequences on the research fields [16]. More work is required to develop in-depth understanding of metallic colloids [17].

Attempts have also been made to synthesize different geometric anisotropic particles and distorted particles in different employed plasma solution processes [18-25] where mainly four strategies remained in utilization i.e., DC plasma discharge in contact with the liquid, DC glow discharge plasma in contact with liquid, pulse plasma discharge inside the liquid, and gas-liquid interface discharge. Quite a few reaction mechanisms proposed by different groups are to be the most probable underlying mechanisms such as plasma electrons [20], hydrogen radicals in liquid [22], aqueous electrons [21] and hydrogen peroxide [18, 19]. Gold nanoplates and nanorods have been synthesized at the surface of solution while spherical-shaped particles inside the solution [22]. Again, probing matter at a length scale comparable to the subwavelength of light can deliver phenomenal optical properties [26, 27] and different phase-controlled syntheses give an

improved catalytic activity of metallic nanostructures as compared to bulk ones [28, 29]. Different tiny-sized particles of gold are discussed elsewhere [30]. Splitting argon atoms switched medium of propagating photons to medium of travelling photons at increasing wavelength where they left inter-state electron gap and entered in the normal medium revealing the glow of light on reaching wavelength in the visible range as discussed elsewhere [31]. Photons characteristic current configure their forcing energy in inter-state electron gap, thus, propagate between states of electrons [32]. The amalgamated atoms bind under generated energy of the targeted atom while executing electron-dynamics as discussed elsewhere [33]; force is being involved to engage the conserved energy. A separate study discussed the mechanism of formation of a triangular-shape gold tiny particle [34]. Carbon atoms of different state bind into tiny grains, grains or crystallites depending on the localized process conditions as discussed elsewhere [35, 36]. Different tiny-sized particles and large-sized particles of gold are discussed elsewhere [37-39] while silver and binary composition of gold and silver are also discussed elsewhere [37]. A detailed study of developing geometric anisotropic particles is presented elsewhere [40]. The origin of different nature atoms in terms of state behavior while dealing liquid state is discussed elsewhere [41]. Again, a recent study reveals the impact of different nature atoms while using their nanoparticles as a nanomedicine application [42].

Present study describes developing gold tiny-sized particles and their different shape large-sized particles while varying the concentration of gold precursor. We briefly discussed the role of varying precursor concentration under fixed process parameters while developing particles of different shapes in locally designed pulse-based electronphoton-solution interface process.

Experimental details:

Solid powder of HAuCl_4 was purchased from Alfa Aesar to obtain the aqueous solution of different molar concentrations. Briefly, aqueous solution of one-gram $\text{HAuCl}_4 \cdot 3\text{H}_2\text{O}$ and ~100 ml DI water was prepared in a glass bottle. This was followed by the preparation of several different molar concentrations by dissolving various amounts of

precursor in DI water in such a way that total quantity of solution obtained for each time was ~100 ml.

Schematic of the setup processed gold solution under different concentrations is shown in Figure 1. A copper capillary with internal diameter ~3 mm (thickness: ~1.5 mm) was used to maintain the flow of argon gas. At the bottom of tube, atoms of flowing argon gas splitted by propagating photons characteristic current. A graphite rod with a width of 1 cm was immersed into the solution known as anode. The distance between copper capillary bottom and solution surface was ~5 mm and was kept constant in all experiments. Distance between graphite rod and copper capillary was set ~4 cm in each experiment. Layout of air-solution interface and electronphoton-solution interface is shown elsewhere [30].

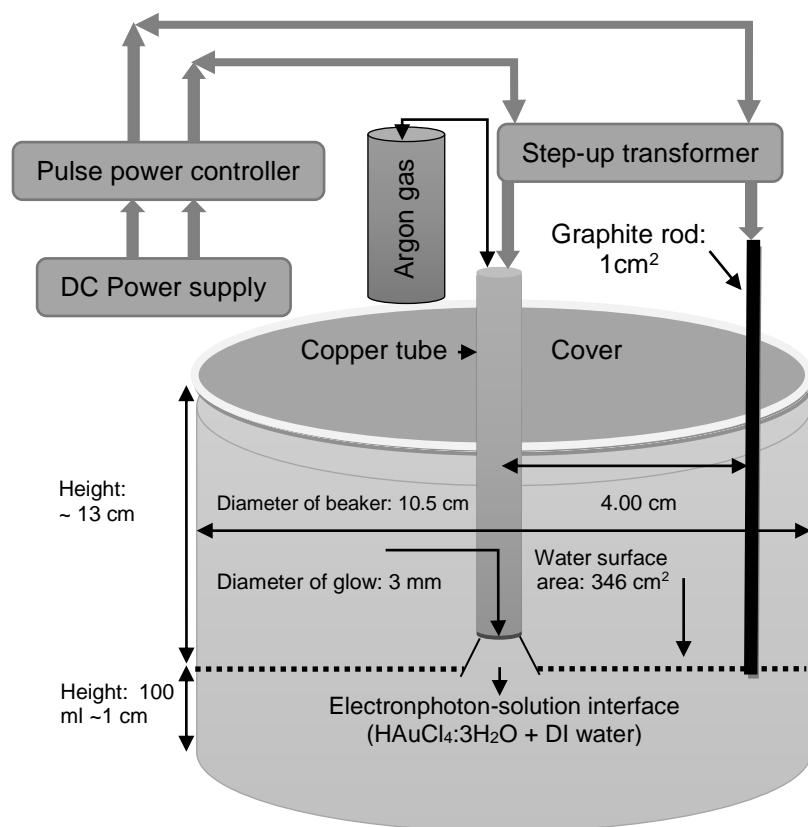


Figure 1: Schematic of pulse-based electronphoton-solution interface process

Bipolar pulse of fixed ON/OFF time was being controlled by the pulse DC power controller (SPIK2000A-20, MELEC GmbH; Germany). Input DC power was provided by SPIK2000A-20. Symmetric-bipolar mode of pulse power controller was employed, and

equal time periods of pulses was set; t_{on} (+/-) = 10 μsec and t_{off} (+/-) = 10 μsec . The input power slightly fluctuated, initially. Fluctuation of input power was highest at the start of the process, dropped to nearly half in a second and remained almost stable in the remaining period where the splitting of inert gas atoms was controlled automatic under the running voltage of 32 volts where current reading was 1.3 amp, which was enhanced ~ 40 times under the application of step-up transformer. The variation in power was 1 % for each concentration of precursor.

Temperature of the solution was recorded with laser-controlled temperature meter (CENTER, 350 Series). In each experiment, temperature was measured at the start ($\sim 20^\circ\text{C}$), middle ($\sim 27^\circ\text{C}$) and at the end ($\sim 37^\circ\text{C}$) of process with $\pm 1^\circ\text{C}$ accuracy. Different molar concentrations were prepared (~ 0.10 mM, ~ 0.30 mM, ~ 0.60 mM, ~ 0.90 mM and ~ 1.20 mM) where duration of the process was set 10 minutes in each experiment. Total argon gas flow rate was 100 sccm, which was maintained through mass flow controller. Different molar concentrations were also prepared (~ 0.07 mM, ~ 0.10 mM, ~ 0.30 mM and ~ 0.60 mM) at argon gas flow rate 50 sccm.

Copper grid covered by carbon film was used and samples were prepared by dip-casting. Samples were placed into Photoplate degasser (JEOL EM-DSC30) for ~ 24 hours to eliminate moisture. Bright field transmission microscope images, selected area photons reflection (SAPR) patterns known as SAED patterns and high-resolution transmission microscope images were taken under the application of microscope known as HR-TEM (JEOL JEM2100F) while operating at 200 kV.

Results and discussion:

Layout of the pulse-based electronphoton-solution interface process is shown in Figure 1 by which nanoparticles and particles developed under different concentration of gold precursor where coalescences of tiny-sized particles occur under certain scheme. At precursor concentration 0.05 mM, spherical-shaped and less-distorted nanoparticles were developed as shown by different bright field transmission microscope images (a-d) in Figures S1 and average size of nanoparticle is remained between 20 to 25 nm. On increasing the precursor concentration to 0.10 mM, the average size of particles increased where many of them developed in geometric anisotropic shape as shown by

bright field transmission microscope images in Figure S2 (a-c). By increasing the precursor concentration from 0.10 mM to 0.30 mM, the average size of different shape of particles further increased where their bright field transmission microscope images are shown in Figure 2 (a) & (b); triangle-, hexagon-, isosceles trapezoid-, rhombus-, pentagon-, rod- and belt-shaped particles developed. Some of the particles show high aspect ratio. The increase in the size of geometric anisotropic particles is mainly related to the increased number of packing of large-sized triangular-shaped tiny particles.

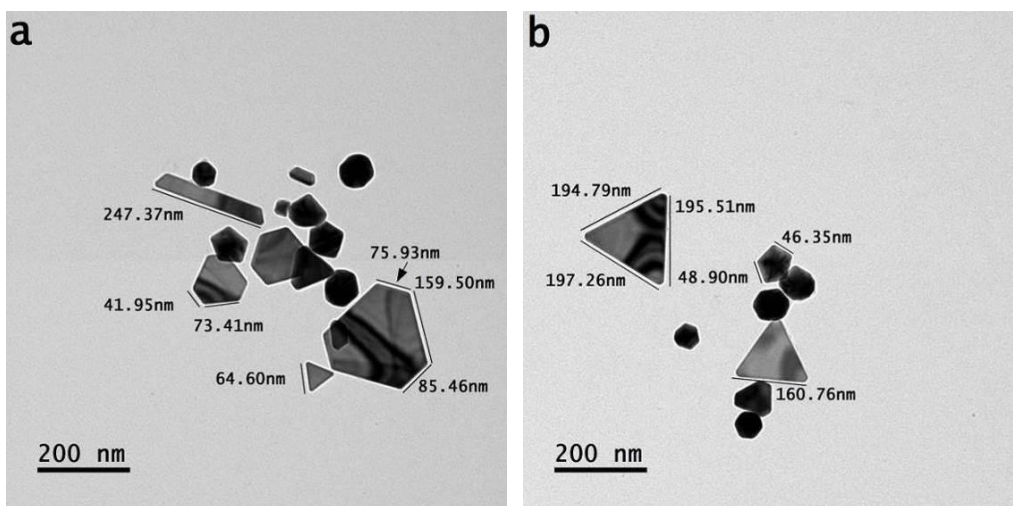
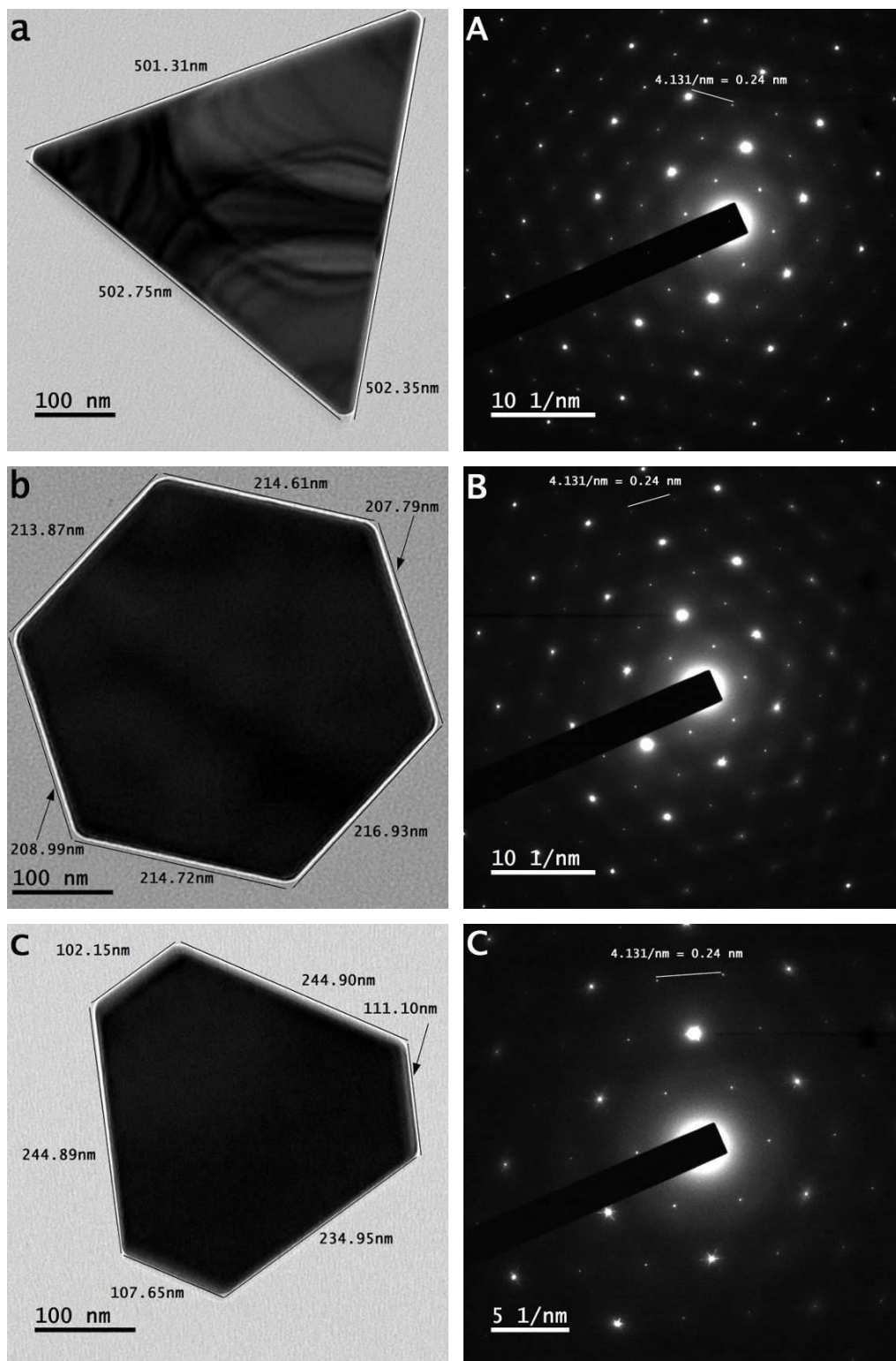
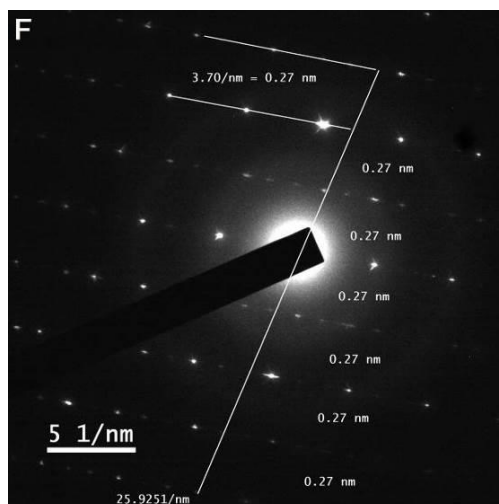
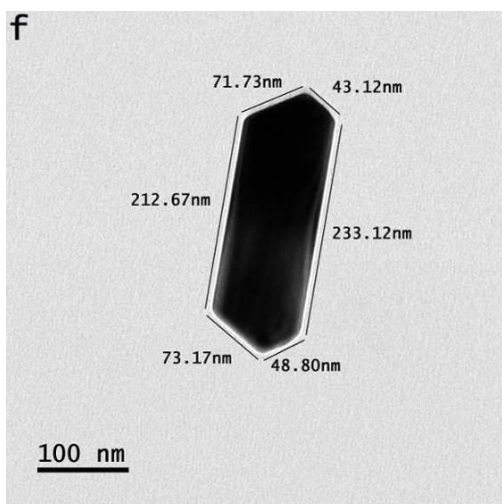
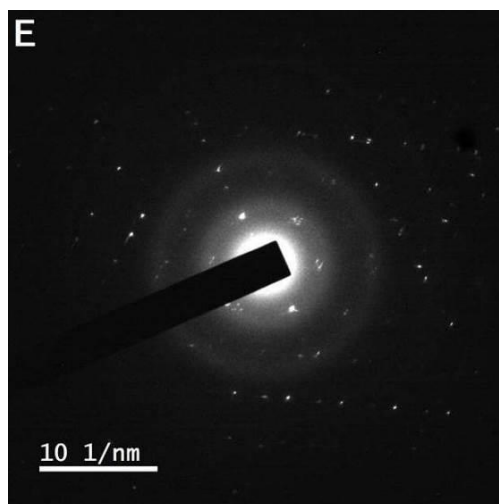
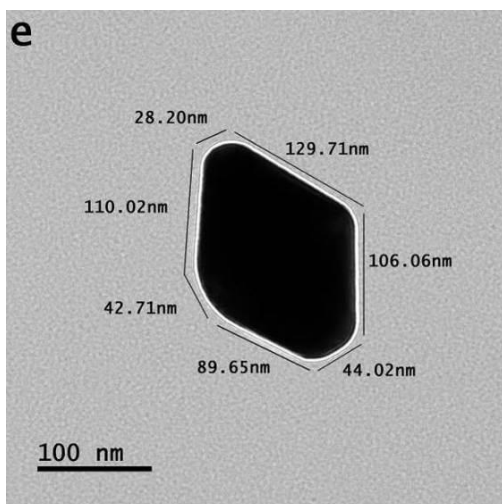
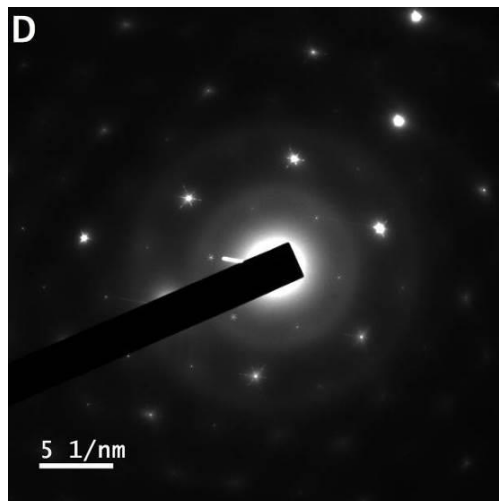
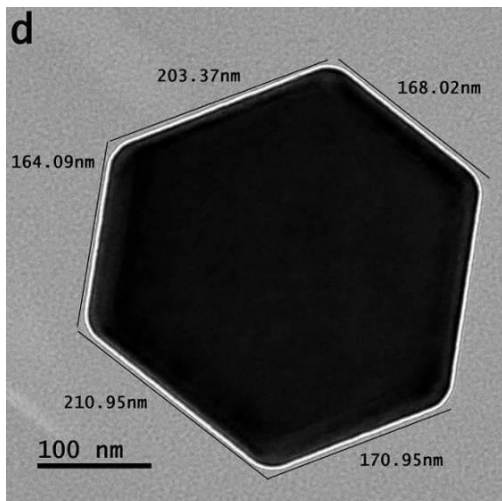


Figure 2: (a) & (b) Bright field transmission microscope images of nanoparticles/particles developed in various geometric anisotropic shapes and distorted shapes; precursor concentration 0.30 mM and argon gas flow rate 100 sccm

Several high aspect ratio shapes are shown by bright field transmission microscope images in Figures 3 (a-f) along with SAPR patterns (in Figure 3A-F); each image shows a unique geometric anisotropic shape of the particle along with its SAPR pattern. SAPR patterns of geometric anisotropic particles indicate one-dimensional structure in the case of bar- and rod-shaped particles, and multi-dimensional structure in the case of triangle- and hexagon-shaped particles. In Figure 3 (g), difference in the sides' length of particles (triangle- and hexagon-shaped particles) is only in the margin of an atom or few atoms, which indicates packing of same size tiny particles where they maintained equal rate of packing from all sides. In some cases, the particles bond *via* their sides (Figure 3h) and in other cases, they are overlaid by one another (Figure 3i). For precursor concentration 0.90 mM, particles of different geometric anisotropic shapes are shown by bright field transmission microscope images in Figure S3 (a-h), which show

the similar features as in the case of particles developed at precursor concentrations 0.10 mM, 0.30 mM and 0.60 mM except that they possess slightly lower aspect ratios.





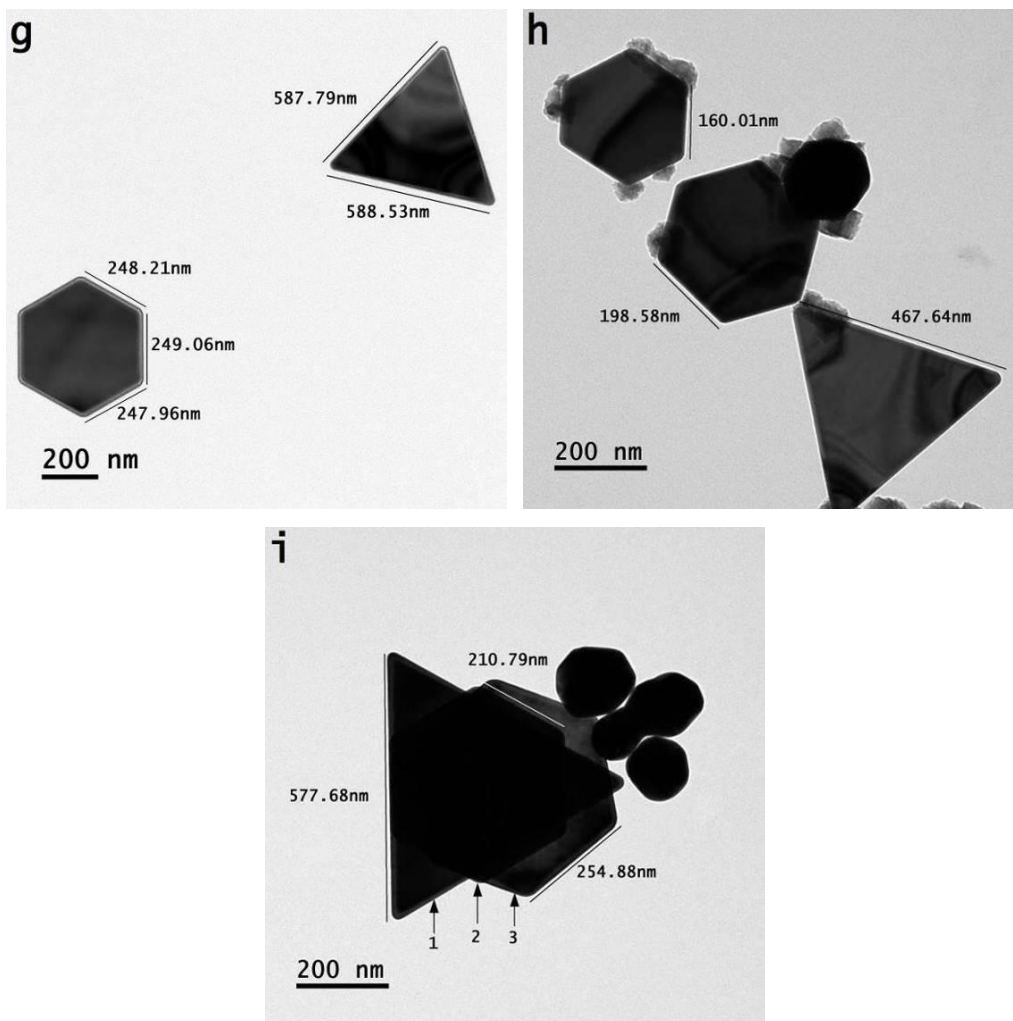
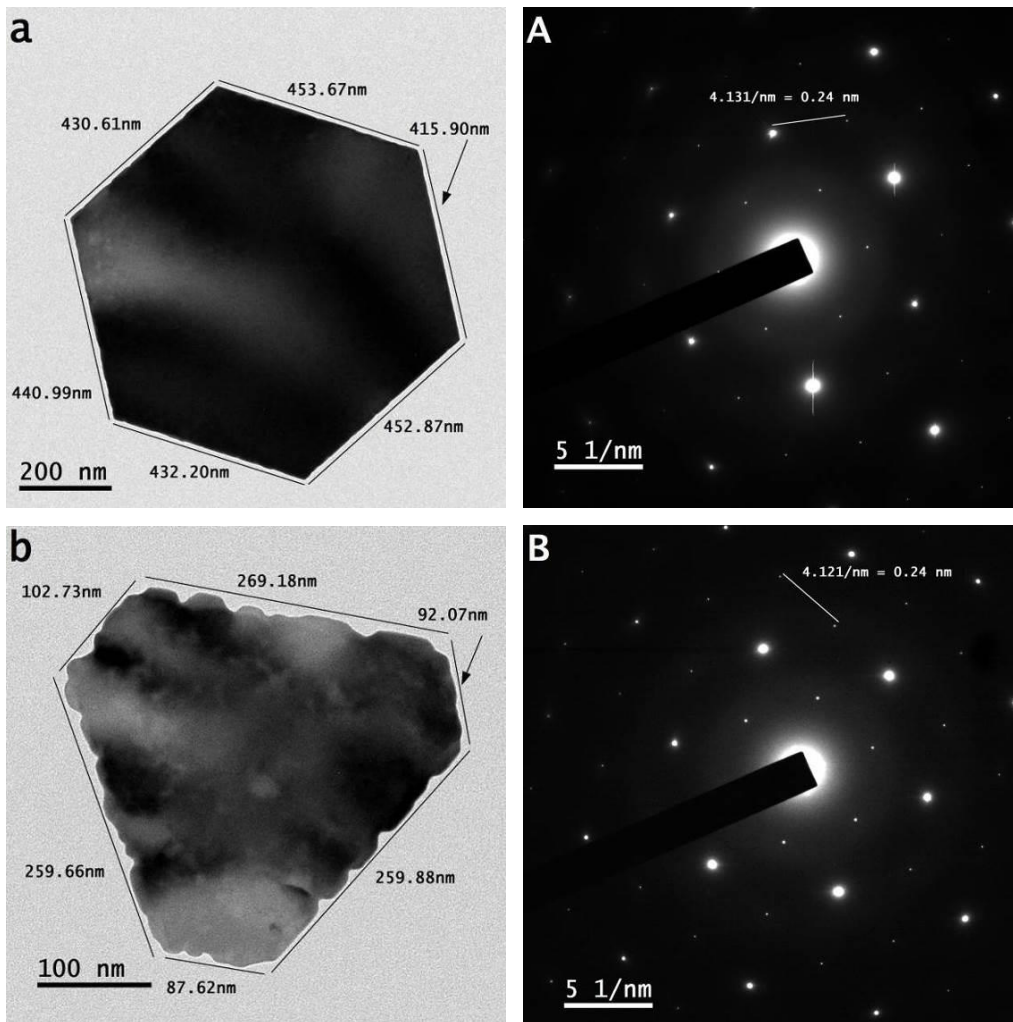
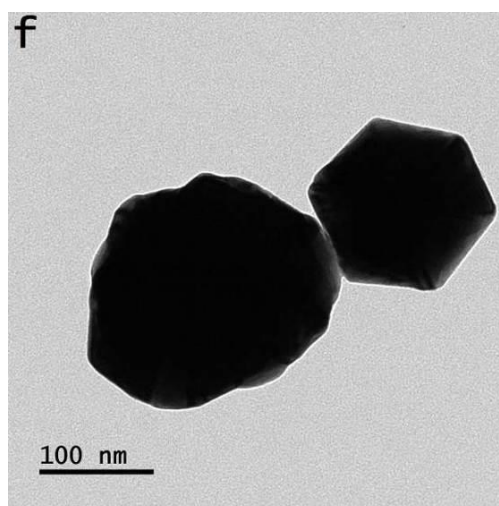
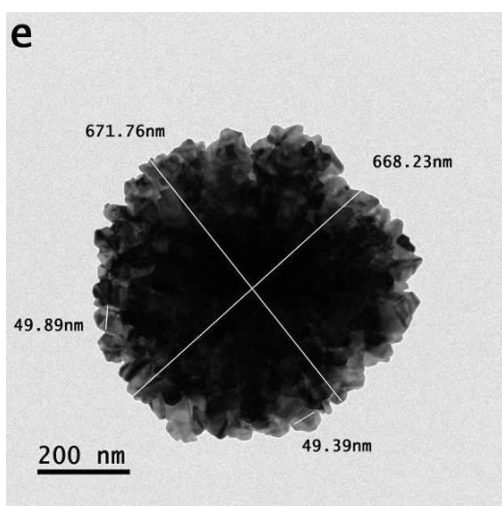
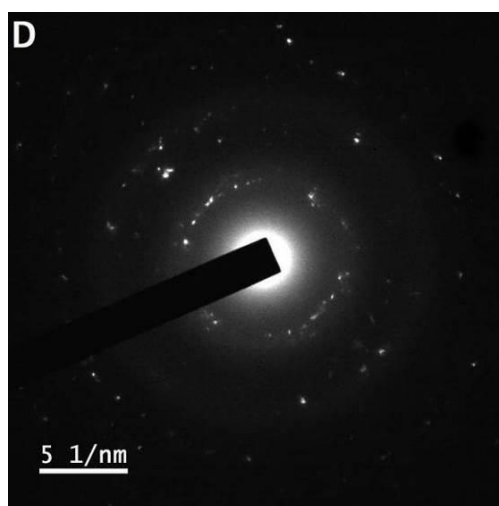
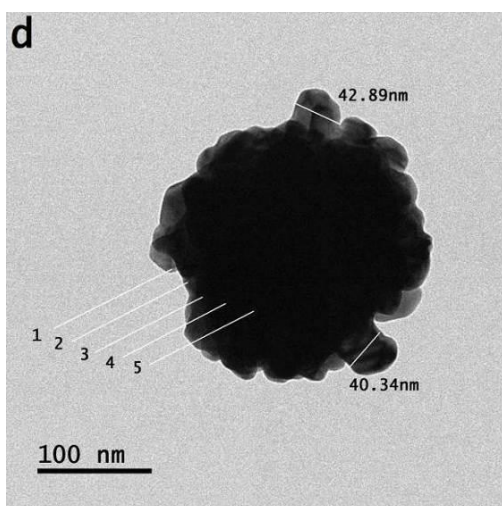
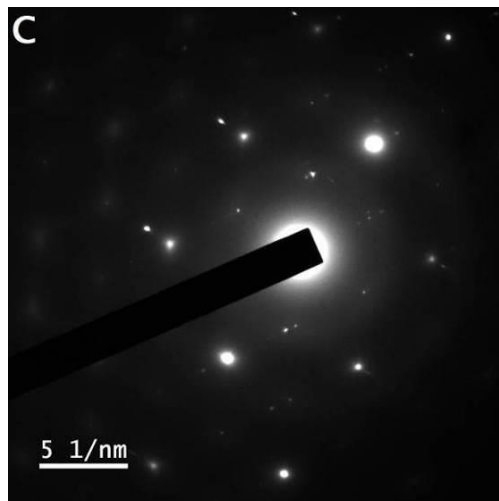
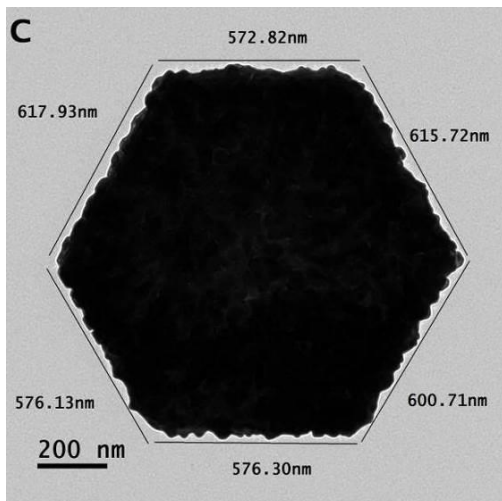


Figure 3: (a-i) Bright field transmission microscope images of particles showing both geometric anisotropic shapes and distorted shapes along with SAPR patterns (A-F); precursor concentration 0.60 mM and argon gas flow rate 100 sccm

At 1.20 mM, very large size tiny particles packed under the exertion of mixed behavior forces which resulted into develop highly-distorted particles as shown by various bright field transmission microscope images in Figure 4 (b-j). Only the particle of hexagonal shape shows anisotropy as shown in Figure 4 (a). SAPR patterns of different shape particles show different structure. The spotted spot of photons in the patterns reflected at the surface of particles (shown in Figures 4a & 4b) covering few elongated atoms indicating uniform structural features (shown in Figure 4A and Figure 4B) as the chosen area of each pattern is only few square nanometers. However, the elongation of atoms in only few square nanometers area in the case of distorted particles (shown in Figures 4c & 4d) is not uniform in terms of structural features as indicated by the

spotted intensity of reflected photons at selected area (shown in Figure 4C and Figure 4D). The packed very large-sized tiny particles don't indicate the one-dimensional structure or multi-dimensional structure of their developed large-sized particle because the shape of developed particle is distorted as shown in Figure 4 (d). Distorted particle shape-like flower is shown in Figure 4 (e) and several particles of identical features are shown in Figure 4 (i). In Figure 4 (e), an average size of tiny particle is 50 nm, which is the cause of their developed particle to deal not only highly disordered structure but no specific morphology also.





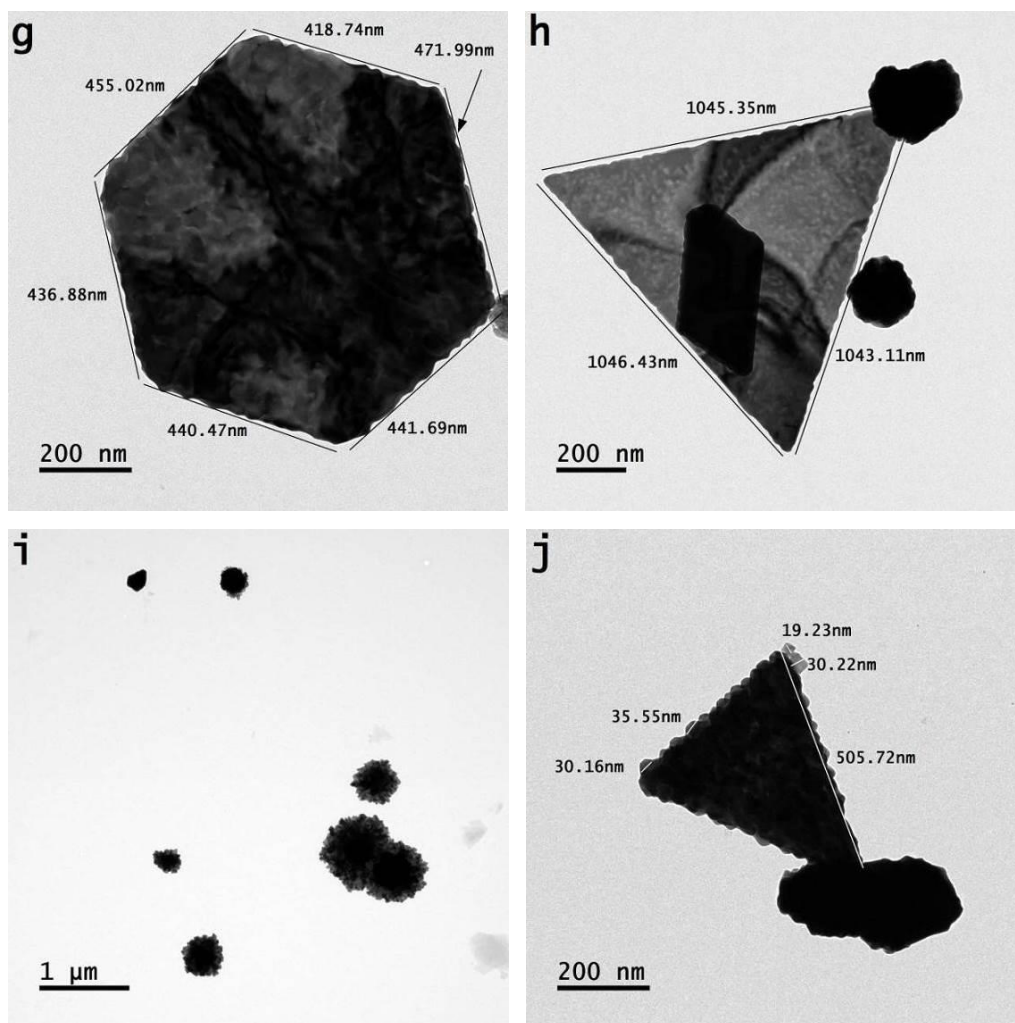


Figure 4: (a-j) Bright field microscope images of particles showing distorted particles (except in 'a')/ SAPR patterns (A-D); precursor concentration 1.20 mM and argon flow rate 100 sccm

The processed solution for different molarities of precursor concentration are shown in Figure S4 (left to right: 0.05 mM, 0.10 mM, 0.30 mM, 0.60 mM, 0.90 mM and 1.20 mM). Besides 100 sccm, solutions were also processed at 50 sccm argon gas flow rate and different colors of the solutions are shown in Figure S5 (left to right: 0.07 mM, 0.10 mM, 0.30 mM and 0.60 mM), whereas, bright field transmission microscope images of nanoparticles and particles are shown in Figures S6-S9. A different color of each solution is related to the overall size and shape of particles along with their quantity, where modes of refraction and reflection of travelling light determine the nature of certain color. Revealing different colors of the colloidal solutions which processed at different molar concentration is appeared to be mainly depended on the scheme of acquired inter-state electron gap in the structure of shaped nanoparticles and particles.

These require the further investigations. Distorted particles as well as geometric anisotropic particles developed at 50 sccm show identical features to the ones developed at 100 sccm. In Figures S6, S7 and S9, some of the shapes developed lengths of sides in the precision of an atom or few atoms, for example, a triangular-shaped particle in Figure S9 (g). Several different shapes of nanoparticles and particles are shown in Figure S10 (a). A triangular-shaped nanoparticle encircled in Figure S10 (a) was dealt with high-resolution transmission microscope image as in Figure S10 (b) where width of elongated atoms of one-dimensional arrays is ~ 0.12 nm. Further details of elongation of atoms of one-dimensional arrays while dealing monolayer triangular-shaped tiny particle is given elsewhere [34]. In the case where developed structure of smooth elements of elongated atoms of one-dimensional arrays in anisotropic particle gained double width is also discussed elsewhere [39]. In SAPR patterns of particles, shapes other than rod or bar, distance between parallel printed intensity spots is ~ 0.24 nm as labeled in Figures 3 (A-C), Figure 4 (A) and Figure S3 (B). On the other hand, the distance between parallel printed intensity spots (which are now intensity lines) in the case of rod (or bar)-shaped particles is ~ 0.27 nm as shown in Figure 3 (F) and in Figure S3 (E). A detail study is given elsewhere [39] presenting the origin of different inter-spacing distance in one-dimensional shaped particles and three-dimensional shaped particles. A separate study discussed the fact of printing intensity spots of reflected photons in shape like lines for one-dimensional structure of particles and in shape like dots for multi-dimensional structure of particles [40].

However, it appears from the feature of different shaped nanoparticles and particles as they are intensively dark in the case synthesized at 50 sccm argon gas flow rate where rate of elongation of atoms of tiny-shaped particles became slightly less due to lower concentration of flowing argon gas, thus, splitting of flowing inert gas atoms to the impingement of their electron streams to the underneath matter is at reduced rate also. However, due to the entering of a smaller number of photons and electron streams into solution (resulted on the splitting of flowing inert gas atoms), the average size of developed nanoparticles and particles is also a bit lower in aspect ratio as compared to those developed at 100 sccm. However, a detailed study is also required for further clarification at this point.

Packing of tiny-shaped particles under exerting surface format force in different geometric anisotropic particles can be drawn from the distributed intensity spots in SAPR pattern. In Figure S3 (C), SAPR pattern also indicates that spotted spots reflected at the surface of structure of hexagonal-shaped particle are under certain pace where photons (not electrons) reflected at the surface of structure of smooth elements of above-positioned particle as well as the underneath one; in the case of latter, photons reflected at the surface of underlying structure while entering through inter-spacing distance of structure of smooth elements of above-positioned particle. Each structure of smooth element is related to the elongated atoms of each one-dimensional array.

On amalgamation of atoms at set precursor concentration, they develop different tiny-sized particles under the application of packets of nano shape energy. At the lowest concentration of precursor (0.05 mM), very fewer gold atoms were available which uplifted to the solution surface but the packet of each nano shape energy possess the same size and shape under set tuned ratio of pulse OFF to ON time as given in the experimental details section. The atoms underneath nano shape energy are insufficient dealing an average size of tiny particle ~ 1.3 nm with no specific geometry of shape. This is because of their not enabling compact monolayer assembly at air-solution interface. Thus, at 0.05 mM (and when unity ratio of pulse OFF to ON time), atoms don't evolve tiny particles in a triangular-shape (Figure 5a₁). Because atoms don't construct one-dimensional arrays in those tiny-sized particles, thus, they don't elongate to form structure of smooth elements as shown in Figure 5 (a₂). They pack under the exertion of non-uniform force resulting into less-distorted and spherical-shaped nanoparticle as shown in Figure 5 (a₃). At fixed bipolar pulse ON/OFF time, increasing the precursor concentration from 0.07 mM to 0.90 mM, many tiny particles developed in a triangular-shape where their size is increased on increasing the precursor concentration. However, in certain regions of solution where tiny-sized particles were not developed in a triangular-shape, they are termed as moderately-disordered tiny particle as shown in Figure 5 (b₁). Such tiny particles do not deal packing under uniform force exerting at the surface of solution. Thus, atoms of such tiny particle didn't elongate uniformly as sketched in Figure 5 (b₂) and termed as moderately-distorted tiny particle. So, such tiny

particles packed under mixed behavior of exerting forces, as a result, a moderately-distorted particle was developed as shown in Figure 5 (b₃).

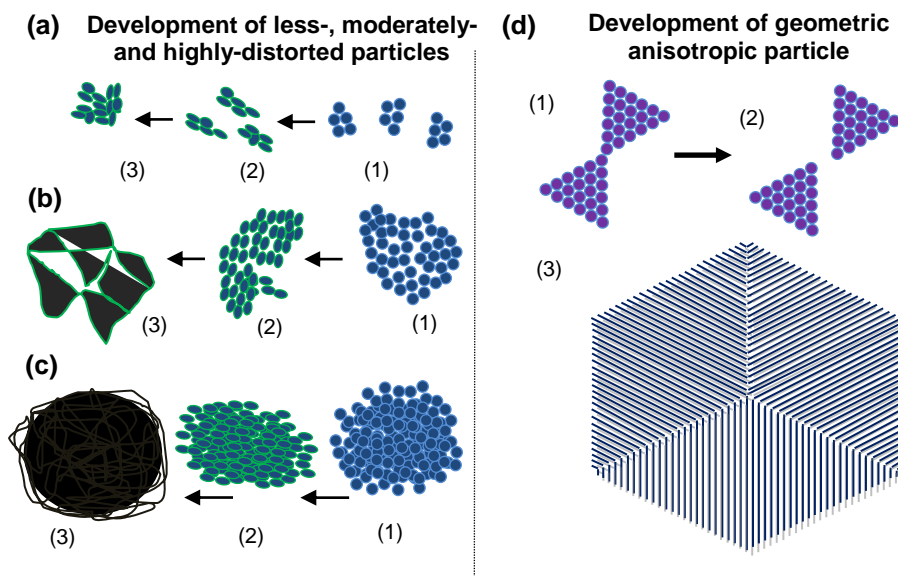


Figure 5: (a₁) Less-disordered tiny particles, (a₂) deformation of ‘less-disordered tiny particles’, (a₃) less-distorted particle; (b₁) Moderately-disordered tiny particle, (b₂) deformation of ‘moderately-disordered tiny particle’ non-uniformly, (b₃) partially-distorted particle; (c₁) Highly-disordered tiny particle, (c₂) deformation of ‘highly-disordered tiny particle’ non-uniformly, (c₃) highly-distorted particle; (d₁) tiny particle of joined triangular-shape, (d₂) separated tiny particle into two equal triangular-shaped tiny particles and (d₃) hexagon-shaped particle (multi-dimensional structure but same in each plane) having structure of smooth elements of elongated atoms of each one-dimensional array

At 1.20 mM, precursor concentration is very large, and assembly developed at solution surface doesn’t deal the compactness in gold atoms since the starting of the process. Due to uplifting of much higher amount of gold atoms to solution surface, it resulted into develop assembly of disorderness instead of monolayer. But, the packets of nano shape energy contained the same size and shape for binding atoms as in the case of processing solutions of lower concentration. Therefore, at initial stage of the process, all the tiny-sized particles developed are highly-disordered and they are large enough in their size. The highly-disordered tiny particles do not evolve in a triangular-shape, so, their structures do not undertake one-dimensional arrays of atoms. A highly-disordered tiny particle is shown in Figure 5 (c₁) where groups of atoms (total atoms: 171) configured along different sides. Thus, a highly-disordered tiny particle elongated along different sides as per exerting the forces along different poles, which is termed as

highly-distorted tiny particle as shown in Figure 5 (c₂). Such large size tiny particles don't pack under the exertion of uniform force resulting into develop highly-distorted particle as shown in Figure 5 (c₃).

A joined triangular-shape tiny particle is shown in Figure 5 (d₁), which was developed under the application of bipolar pulse while processing the solution of gold under certain precursor concentration. The joined triangular-shape tiny particles separated at the point of connection under the exertion of force along opposite poles as shown Figure 5 (d₂). Six elongated tiny particles of different regions at solution surface located at equidistant to the centre of packing nucleated structure of hexagonal-shaped particle at the centre of pulse-based electron-photon-solution interface and packing of several such tiny-shaped particles while retaining intact initially originated the symmetry resulting into develop hexagonal-shaped particle as shown in Figure 5 (d₃) where the width of each structure of smooth element along with their inter-spacing distance is almost the same as in the case of particle shown in Figure S10 (b); the width is measured with original scale marker. Thickness of each structure of smooth element is appeared to be the same as the resulted width of each elongated one-dimensional array of gold atoms (~0.12 nm). A structure of smooth element is related to elongated atoms of one-dimensional array when they are in their certain transition state [34]. A further detail of developing various geometric anisotropic particles is given elsewhere [41].

Under very high concentration of gold precursor (1.20 mM), average size of tiny particles was 50 nm at the start of process and on prolonging the process time, tiny particles resulted in decreased size as discussed elsewhere [30]. Therefore, the geometric anisotropic particle shown in Figure 4 (a) is due to smaller size tiny particles developed at the later stage of the process. This indicates that by increasing the process duration, the favorable conditions prevailed, and tiny particles of a non-triangular-shape turned into a triangular-shape under the favorable conditions of the process. Therefore, initial concentration of precursor is not the only parameter controlling the size and shape of tiny particles and it depends on time-to-time change in the precursor concentration also. Origin of gas and solid behavior of atoms discussed elsewhere [42]. As per nature of atoms of tiny-sized particles, they can be a defective

nanomedicine instead of being effective [43]. Developing hard coating is under the switched force-energy behaviors of different nature atoms [44].

It has been pointed out that upto certain numbers of atoms, tiny particles are developed in hcp structures [45] and tiny particle size upto a point shows metallic character [46]. It has been stated that besides geometry and entropy, progress research efforts are considering the use of geometry and entropy to explain not only structure but dynamics also [47] and disordered jammed configuration is not the only one in any known protocol but there are also ordered metrics, which characterize the order of packing [48]. A study on size-controlled gold nanoparticles while synthesizing in photochemical process has been given elsewhere [49]. From the application point of view, nanoparticles and particles having distorted shapes show potential in various catalytic applications, whereas, those in geometric anisotropic shapes indicate potential to use as ultra-high-speed devices along with applications in diversified areas, in optics, medical and photonic devices, etc.

Conclusions:

In pulsed-based electron-photon-solution interface process, the development of geometric anisotropic gold particles depends on the features of their assembling tiny-sized particles; distorted particles developed when tiny particles of a non-triangular-shape coalesced or packed. The developing tiny particles of different sizes with certain features again depend on the amount of precursor concentration. A certain amount of precursor concentration under the fixed ratio of bipolar pulse OFF to ON time results into develop many tiny particles having a triangular-shape. Increasing the molar concentration of gold precursor from 0.05 mM to 1.20 mM, average size of gold tiny particles increases from 1.3 nm (approx.) to 50 nm (approx.). At 0.05 mM, tiny-sized particles do not develop in a triangular-shape. Packing of such tiny particles results into develop less-distorted spherical-shaped nanoparticles. At 0.07 to 0.90 mM, many tiny-sized particles develop in a triangular-shape where have a large number at 0.30 mM and 0.60 mM. So, this is how it is in the case of developing geometric anisotropic particles. At 1.20 mM, many tiny-sized particles do not develop in a triangular-shape and their packing resulted into develop distorted particles also where their SAPR

patterns show disordered structure. The decreasing argon gas flow rate from 100 sccm to 50 sccm doesn't influence the overall behavior of particles' shape. The color of the solution is changed due to the overall impact of configuring modes of refraction and reflection of incident light where scheme of inter-state electron gaps belonging to structure of elongated atoms in different shaped particles may be the main cause.

Acknowledgements:

Mubarak Ali thanks National Science Council (now MOST) Taiwan (R.O.C.) for awarding postdoctorship: NSC-102-2811-M-032-008 (August 2013- July 2014). Authors wish to thank Dr. Kamatchi Jothiramalingam Sankaran, National Tsing Hua University and Mr. Vic Chen, Tamkang University, Taiwan (R.O.C.) for assisting in transmission microscope operation. Mubarak Ali greatly appreciates useful suggestions of Dr. M. Ashraf Atta while writing the paper.

References:

1. Daniel, M-C, Astruc D (2004) Gold Nanoparticles: Assembly, Supramolecular Chemistry, Quantum-Size-Related Properties, and Applications toward Biology, Catalysis, and Nanotechnology. *Chem. Rev.* 104; 293-346.
2. Brust M, Walker M, Bethell D, Schiffrin D J, Whyman R (1994) Synthesis of Thiol-derivatised Gold Nanoparticles in a Two-phase Liquid-Liquid System. *J. Chem. Soc., Chem. Commun.* 801-802.
3. Whetten RL; Khoury JT, Alvarez MM, Murthy S, Vezmar I, Wang ZL, Stephens PW, Cleveland, CL, Luedtke WD, Landman U (1996) Nanocrystal Gold Molecules. *Adv. Mater.* 8; 428-433.
4. Link, S, El-Sayed, MA (2000) Shape and size dependence of radiative, nonradiative and photothermal properties of gold nanocrystals. *Inter. Rev. Phys. Chem.* 19; 409-453.
5. Brown LO, Hutchison JE (2001) Formation and Electron Diffraction Studies of Ordered 2-D and 3-D Superlattices of Amine-Stabilized Gold Nanocrystals. *J. Phys. Chem. B* 105;8911-8916.

6. Whitesides GM, Boncheva M (2002) Beyond molecules: Self-assembly of mesoscopic and macroscopic components. *Proc. Natl. Acad. Sci. U.S.A.* 99; 4769-4774.
7. Brust M, Kiely CJ (2002) Some recent advances in nanostructure preparation from gold and silver particles: a short topical review. *Colloids and Surfaces A: Physicochem. Eng. Aspects* 202; 175-186.
8. Huang J, Kim F, Tao AR, Connor S, Yang P (2005) Spontaneous formation of nanoparticle stripe patterns through dewetting. *Nat. Mater.* 4; 896-900.
9. Glotzer SC, Horsch MA, Iacovella CR, Zhang Z, Chan ER, Zhang X (2005) Self-assembly of anisotropic tethered nanoparticle shape amphiphiles. *Curr. Opin. Colloid Interface Sci.* 10;287-295.
10. Glotzer SC, Solomon MJ (2007) Anisotropy of building blocks and their assembly into complex structures. *Nature Mater.* 6; 557-562.
11. Shaw CP, Fernig DG, Lévy R (2011) Gold nanoparticles as advanced building blocks for nanoscale self-assembled systems. *J. Mater. Chem.* 21; 12181-12187.
12. Vanmaekelbergh D (2011) Self-assembly of colloidal nanocrystals as route to novel classes of nanostructured materials. *Nano Today* 6;419-437.
13. Liu N, Tang ML, Hentschel M, Giessen H, Alivisatos AP (2011) Nanoantenna-enhanced gas sensing in a single tailored nanofocus. *Nat. Mater.* 10; 631-637.
14. Mulvaney P (1996) Surface Plasmon Spectroscopy of Nanosized Metal Particles. *Langmuir* 12: 788-800.
15. Lofton C, Sigmund W (2005) Mechanisms controlling crystal habits of gold and silver colloids. *Adv. Funct. Mater.* 15; 1197-1208.
16. Tao A, Sinsermsuksakul P, Yang P (2006) Polyhedral Silver Nanocrystals with Distinct Scattering Signatures. *Angew. Chem. Int. Ed.* 45; 4597-4601.
17. Millstone JE, Hurst SJ, Métraux GS, Cutler JI, Mirkin CA (2009) Colloidal Gold and Silver Triangular Nanoprisms. *Small* 5; 646-664.
18. Mariotti D, Patel J, Švrček V, Maguire P (2012) Plasma –Liquid Interactions at Atmospheric Pressure for Nanomaterials Synthesis and Surface Engineering. *Plasma Process. Polym.* 9; 1074-1085.

19. Patel J, Němcová L, Maguire P, Graham WG, Mariotti D (2013) Synthesis of surfactant-free electrostatically stabilized gold nanoparticles by plasma –induced liquid Chemistry. *Nanotechnology* 24;245604-14.
20. Huang X, Li Y, Zhong X (2014) Effect of experimental conditions on size control of Au nanoparticles synthesized by atmospheric microplasma electrochemistry. *Nanoscale Research Lett.* 9; 572-578.
21. Saito N, Hieda J, Takai O (2009) Synthesis process of gold nanoparticles in solution plasma. *Thin Solid Films* 518; 912-917.
22. Furuya K, Hirowatari Y, Ishioka T, Harata A (2007) Protective Agent-free Preparation of Gold Nanoplates and Nanorods in Aqueous H₂AuCl₄ Solutions Using Gas–Liquid Interface Discharge. *Chem. Lett.* 36; 1088-1089.
23. Hieda J, Saito N, Takai O (2008) Exotic shapes of gold nanoparticles synthesized using plasma in aqueous solution. *J. Vac. Sci. Technol. A* 26;854-856.
24. Shirai N, Uchida S, Tochikubo F (2014) Synthesis of metal nanoparticles by dual plasma electrolysis using atmospheric dc glow discharge in contact with liquid. *Jpn. J. Appl. Phys.* 53; 046202-07.
25. Baba K, Kaneko T, Hatakeyama R (2009) Efficient Synthesis of Gold Nanoparticles Using Ion Irradiation in Gas–Liquid Interfacial Plasmas. *Appl. Phys. Exp.* 2;035006-08.
26. Liu Y, Zhang X (2011) Metamaterials: a new frontier of science and technology. *Chem. Soc. Rev.* 40; 2494-2507.
27. Kuzyk A, et al. (2012) DNA-based self-assembly of chiral plasmonic nanostructures with tailored optical response. *Nature* 483; 311-314.
28. Kim J, Lee Y, Sun S (2010) Structurally ordered FePt nanoparticles and their enhanced catalysis for oxygen reduction reaction. *J. Am. Chem. Soc.* 132; 4996-4997.
29. Kusada K, et al. (2013) Discovery of face-centered-cubic ruthenium nanoparticles: facile size-controlled synthesis using the chemical reduction method. *J. Am. Chem. Soc.* 135; 5493-5496.

30. Ali, M., Lin, I –N. The effect of the Electronic Structure, Phase Transition and Localized Dynamics of Atoms in the formation of Tiny Particles of Gold. <http://arxiv.org/abs/1604.07144> (last version)
31. Ali, M. Atoms of electron transition deform or elongate but do not ionize while inert gas atoms split. <http://arxiv.org/abs/1611.05392> (last version)
32. Ali, M. Revealing the Phenomena of Heat and Photon Energy on Dealing Matter at Atomic level. <http://www.preprints.org/manuscript/201701.0028/v10>
33. Ali, M. Structure evolution in atoms of solid state dealing electron transitions. <http://arxiv.org/abs/1611.01255> (last version)
34. Ali, M. The study of tiny-shaped particle dealing localized gravity at solution surface. <http://arxiv.org/abs/1609.08047> (last version)
35. Ali M, Lin, I –N. Phase transitions and critical phenomena of tiny grains carbon films synthesized in microwave-based vapor deposition system. <http://arXiv.org/abs/1604.07152> (last version)
36. Ali M, Ürgen, M (2017) Switching dynamics of morphology-structure in chemically deposited carbon films-a new insight. *Carbon*, 122; 653-663.
37. Ali M, Lin, I –N, Yeh, C -Y. Tapping Opportunity of Tiny-Shaped Particles and Role of Precursor in Developing Shaped Particles. *NANO* 13 (7) (2018) 1850073 (16 pages). <https://doi.org/10.1142/S179329201850073X>
38. Ali M, Lin, I –N. Controlling morphology-structure of particles at different pulse rate, polarity and effect of photons on structure. <http://arxiv.org/abs/1605.04408> (last version)
39. Ali M, Lin, I –N. Formation of tiny particles and their extended shapes –Origin of physics and chemistry of materials. <http://arxiv.org/abs/1605.09123> (last version)
40. M. Ali, I –N. Lin, Precise Structural Identification of Different Shapes of High Aspect Ratio Gold Particles. (submitted for consideration)
41. Ali, M, Lin, I –N, Yeh, C –J. Predictor packing in developing unprecedented shaped colloidal particles. <https://www.preprints.org/manuscript/201801.0039/v4> (accepted in NANO)
42. Ali, M. Why Atoms of Some Elements are in Gas State and Some in Solid State, but Carbon Works on Either Side. https://www.researchgate.net/profile/Mubarak_Ali5

43. Ali, M. (2017) Nanoparticles-Photons: Effective or Defective Nanomedicine. *J. Nanomed. Res.* 5(6); 00139.
44. Ali, M, Hamzah, E, Toff, M R M. Hard Coating is Because of Oppositely Worked Force-Energy Behaviors of Atoms. <https://www.preprints.org/manuscript/201802.0040/> (last version)
45. Negishi Y, et al. (2015) A Critical Size for Emergence of Nonbulk Electronic and Geometric Structures in Dodecanethiolate-Protected Au Clusters. *J. Am. Chem. Soc.* 137; 1206-1212.
46. Moscatelli A (2015) Gold nanoparticles: Metallic up to a point. *Nature Nanotechnol.* DOI:10.1038/nnano.2015.16.
47. Manoharan, V N (2015) Colloidal matter: Packing, geometry, and entropy, *Science* 349; 1253751.
48. Atkinson S, Stillinger, F H, Torquato S (2015) Existence of isostatic, maximally random jammed monodisperse hard-disk packings, *Proc. Natl. Acad. Sci. U.S.A.* 111; 18436-18441.
49. Kim, J -H, Lavin, B W, Burnett, R D, Boote, B W (2011) Controlled synthesis of gold nanoparticles by fluorescent light irradiation, *Nanotechnology* 22; 285602.

Authors' biography:



Mubarak Ali graduated from University of the Punjab with B.Sc. (Phys& Maths) in 1996 and M.Sc. Materials Science with distinction at Bahauddin Zakariya University, Multan, Pakistan (1998); thesis work completed at Quaid-i-Azam University Islamabad. He gained Ph.D. in Mechanical Engineering from Universiti Teknologi Malaysia under the award of Malaysian Technical Cooperation Programme (MTCP;2004-07) and postdoc in advanced surface technologies at Istanbul Technical University under the foreign fellowship of The Scientific and Technological Research Council of Turkey (TÜBİTAK; 2010). He completed another postdoc in the field of nanotechnology at Tamkang University Taipei (2013-2014) sponsored by National Science Council now M/o Science and Technology, Taiwan (R.O.C.). Presently, he is working as Assistant Professor on tenure track at COMSATS University Islamabad (previously known as COMSATS Institute of Information Technology), Islamabad, Pakistan (since May 2008) and prior to that worked as assistant director/deputy director at M/o Science & Technology (Pakistan Council of Renewable Energy Technologies, Islamabad; 2000-2008). He was invited by Institute for Materials Research, Tohoku University, Japan to deliver scientific talk. He gave several scientific talks in various countries. His core area of research includes materials science, physics & nanotechnology. He was also offered the merit scholarship for the PhD study by the Government of Pakistan, but he couldn't avail. He is author of several articles available at <https://scholar.google.com.pk/citations?hl=en&user=UYjvhDwAAAAJ>, https://www.researchgate.net/profile/Mubarak_Ali5.



I-Nan Lin is a senior professor at Tamkang University, Taiwan. He received the Bachelor degree in physics from National Taiwan Normal University, Taiwan, M.S. from National Tsing-Hua University, Taiwan, and the Ph.D. degree in Materials Science from U. C. Berkeley in 1979, U.S.A. He worked as senior researcher in Materials Science Centre in Tsing-Hua University for several years and now is faculty in Department of Physics, Tamkang University. Professor Lin has more than 200 referred journal publications and holds top position in his university in terms of research productivity. Professor I-Nan Lin supervised several PhD and Postdoc candidates around the world. He is involved in research on the development of high conductivity diamond films and on the transmission microscopy of materials.

Supplementary Materials:

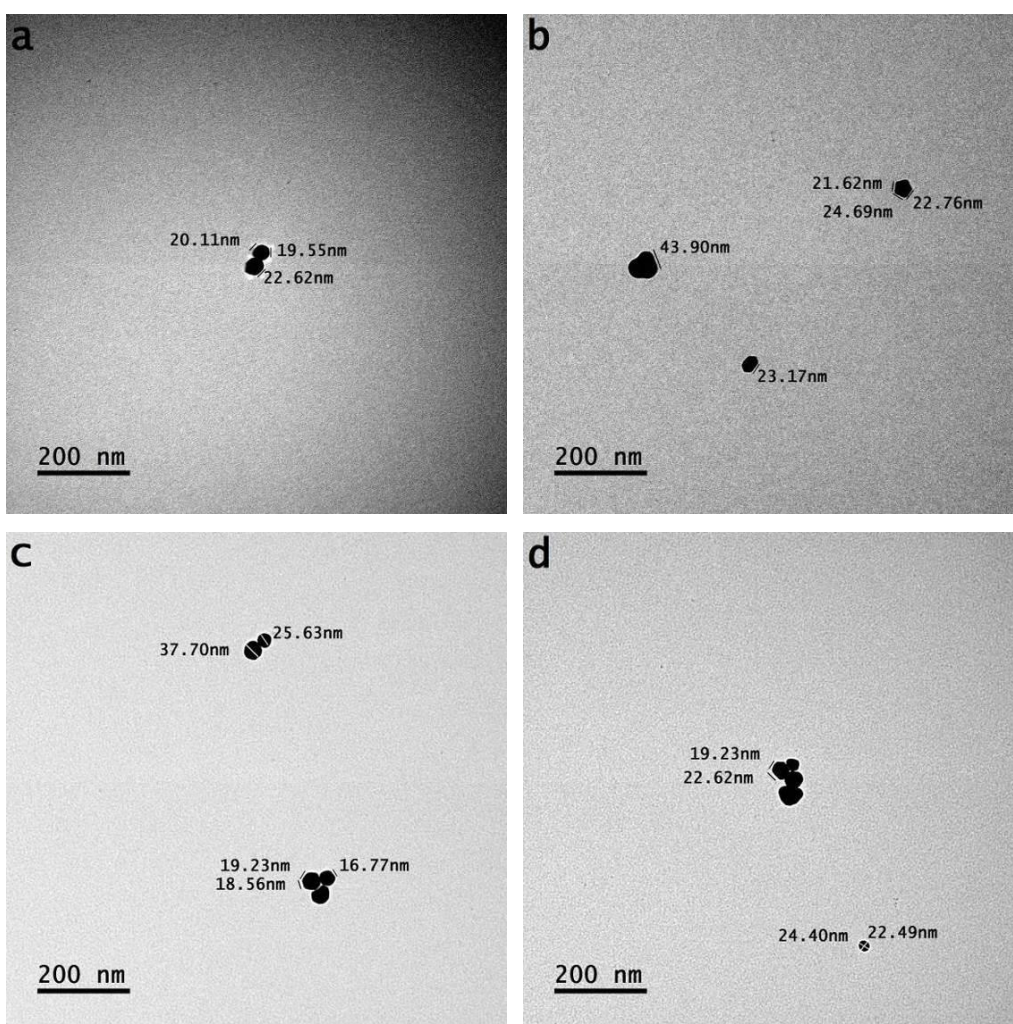


Figure S1: (a-d) Bright field transmission microscope images of nanoparticles showing various less-distorted shapes; precursor concentration 0.05 mM and argon gas flow rate 100 sccm

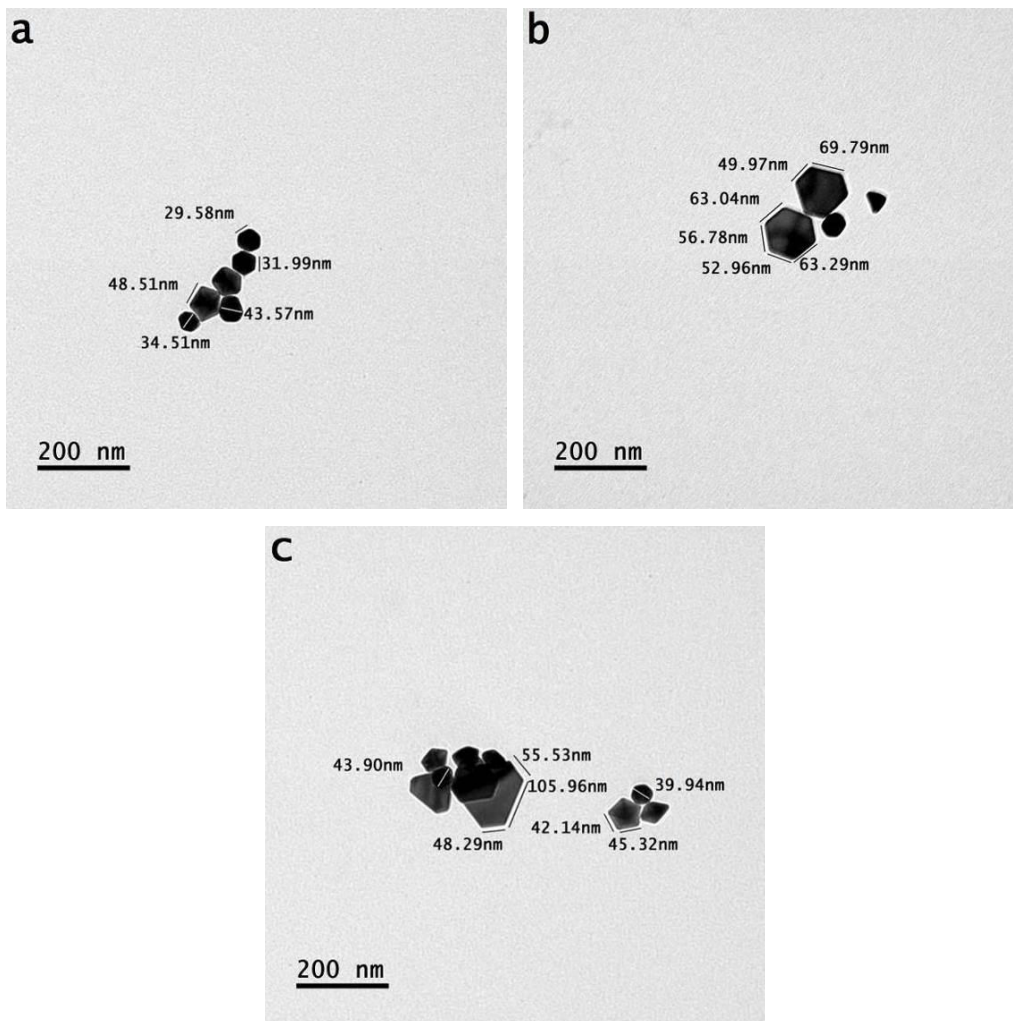
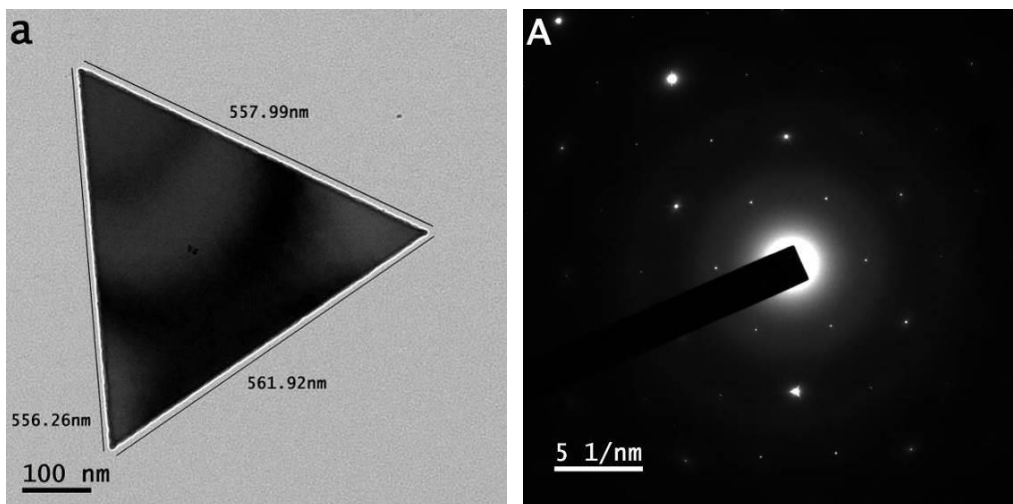
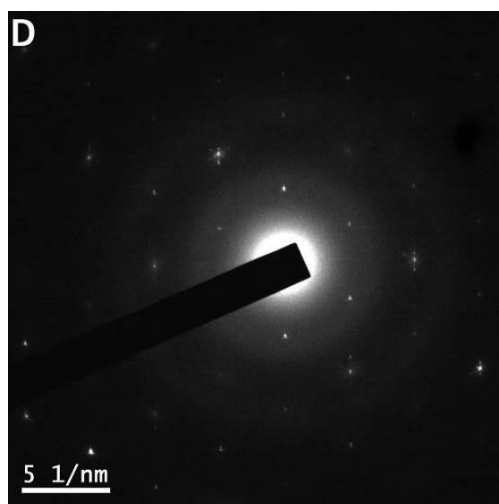
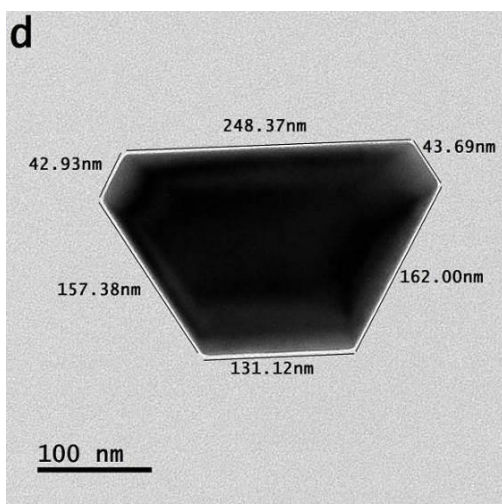
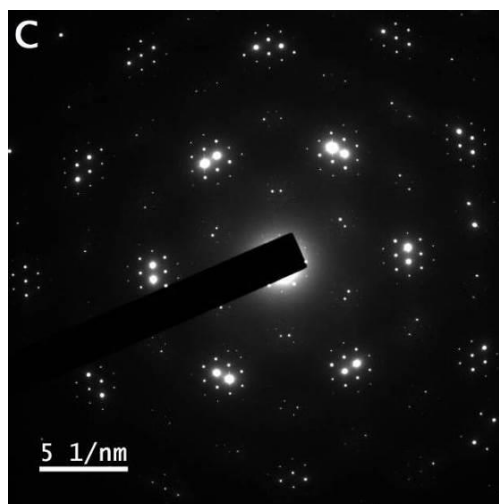
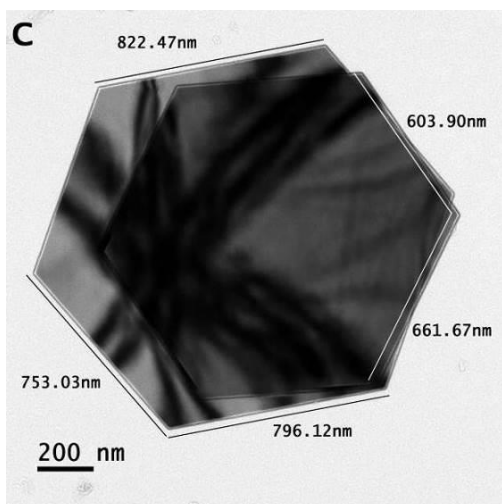
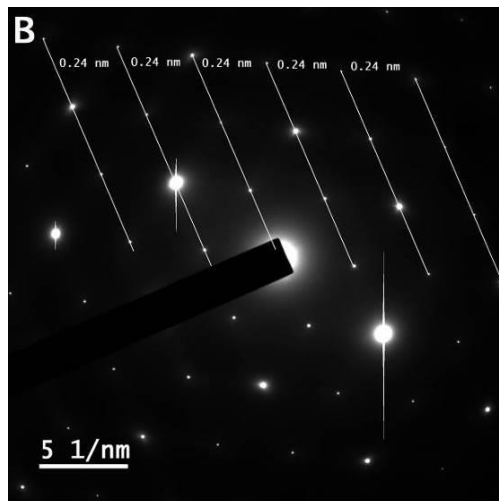
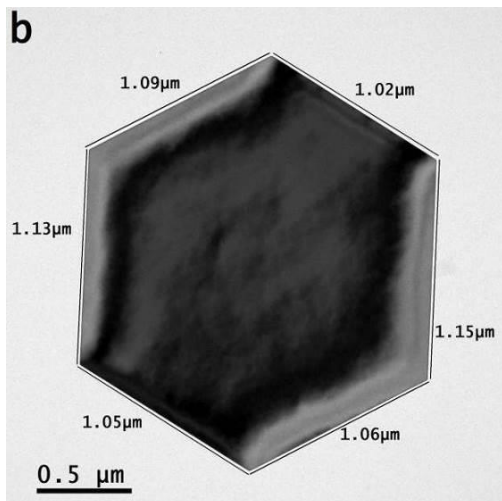


Figure S2: Bright field transmission microscope images of nanoparticles showing both geometric anisotropic shapes and distorted shapes; precursor concentration 0.10 mM and argon flow rate 100 sccm





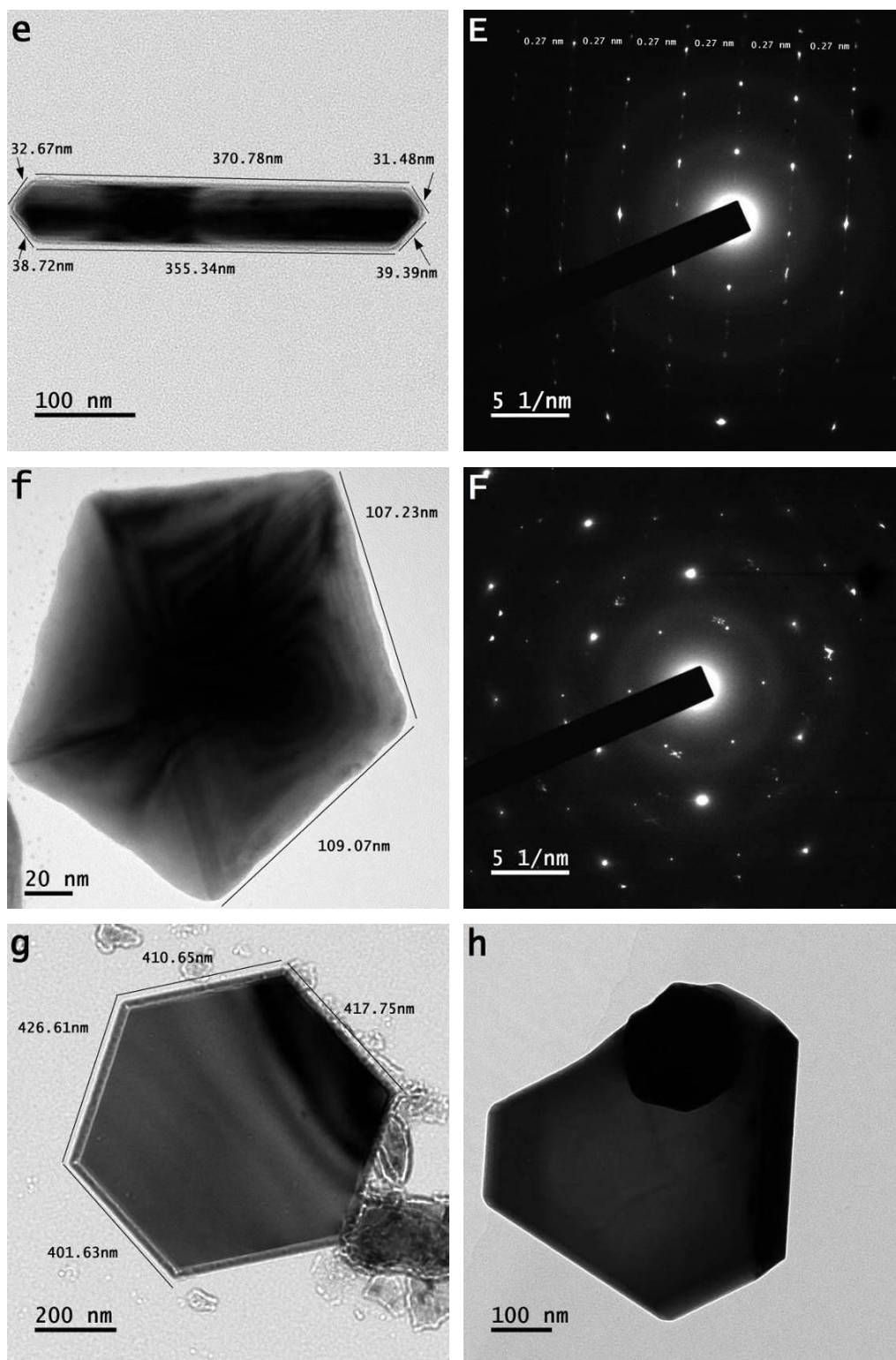


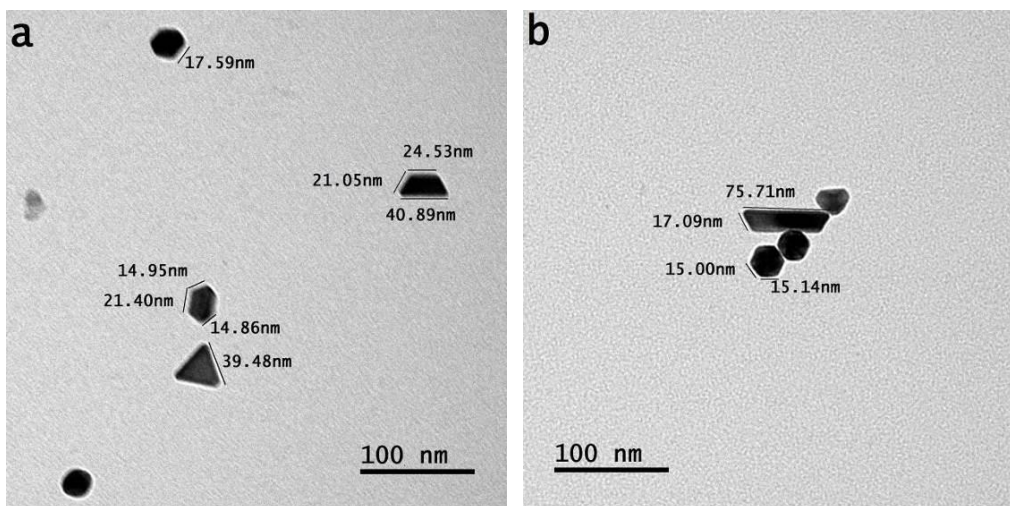
Figure S3: Bright field microscope images of particles showing both anisotropic and distorted shapes along with SAPR patterns (A-F); precursor concentration 0.90 mM and argon flow rate 100 sccm



Figure S4: Different color of solutions processed under different molar concentration of precursor (0.05 mM, 0.10 mM, 0.30 mM, 0.60 mM, 0.90 mM and 1.20 mM, left to right) and argon flow rate 100 sccm



Figure S5: Different color of solutions processed under different molar concentration of precursor (0.07 mM, 0.10 mM, 0.30 mM and 0.60 mM, left to right) and argon flow rate 50 sccm



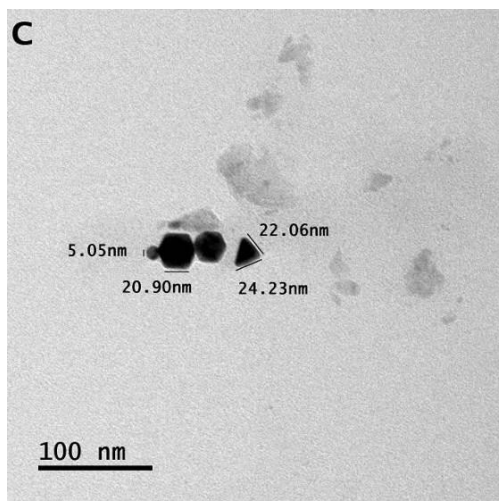


Figure S6: Bright field transmission microscope images of nanoparticles showing both geometric anisotropic shapes and distorted shapes; precursor concentration 0.07 mM and argon flow rate 50 sccm

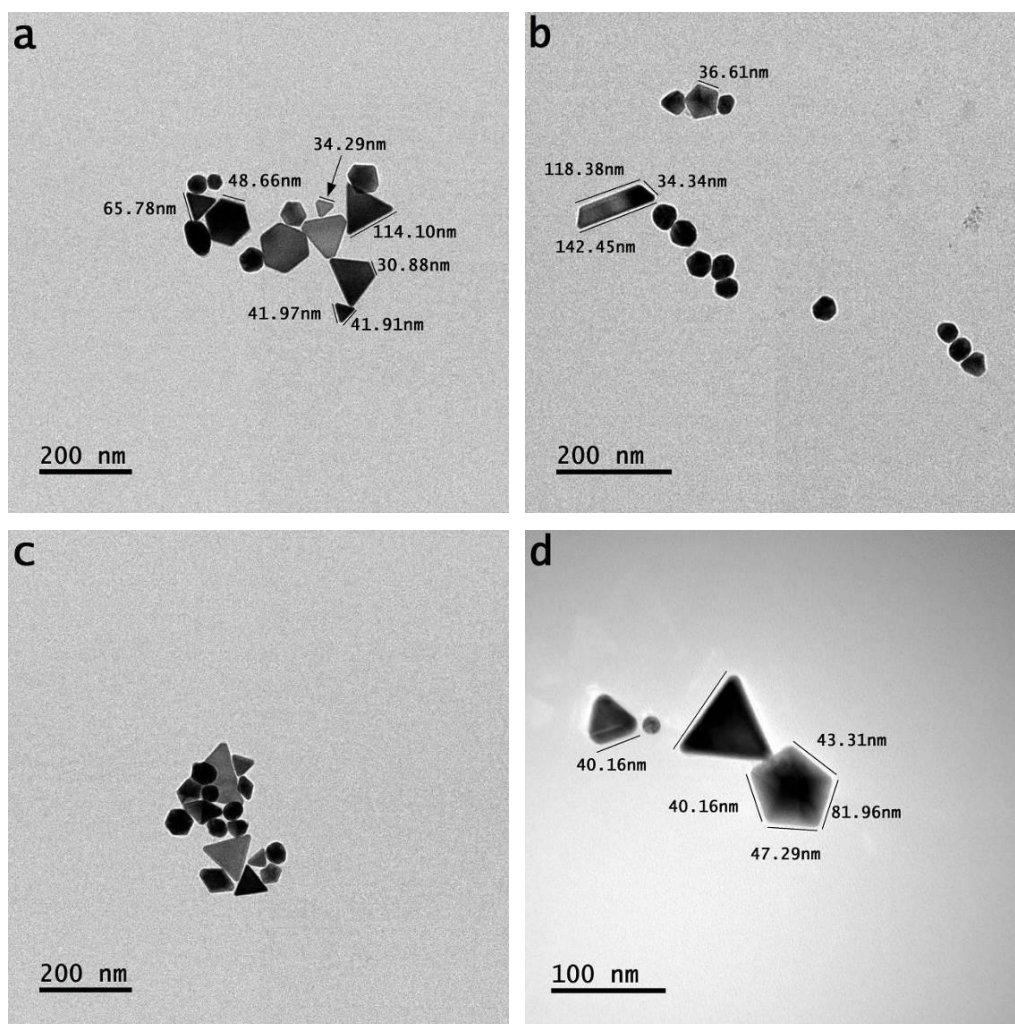


Figure S7: Bright field transmission microscope images of nanoparticles showing both geometric anisotropic shapes and distorted shapes; precursor concentration 0.10 mM and argon flow rate 50 sccm

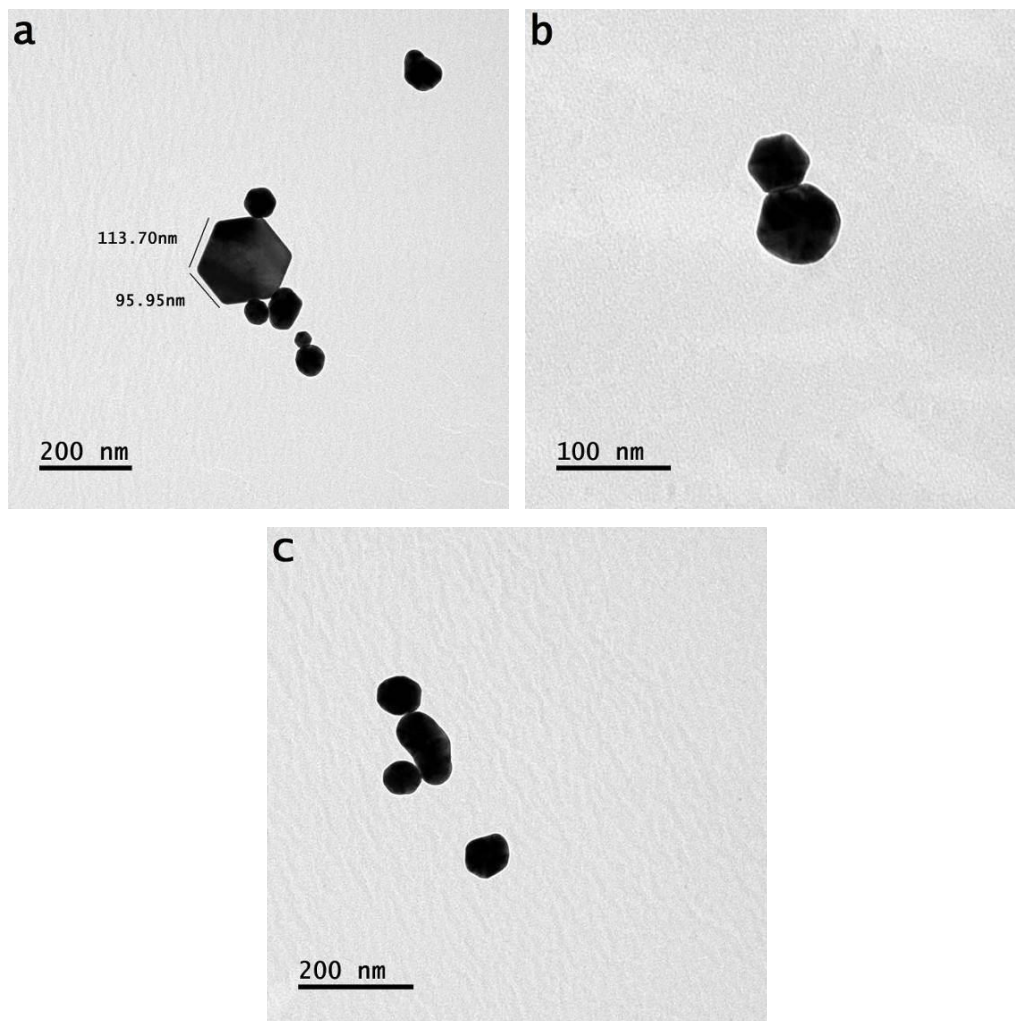
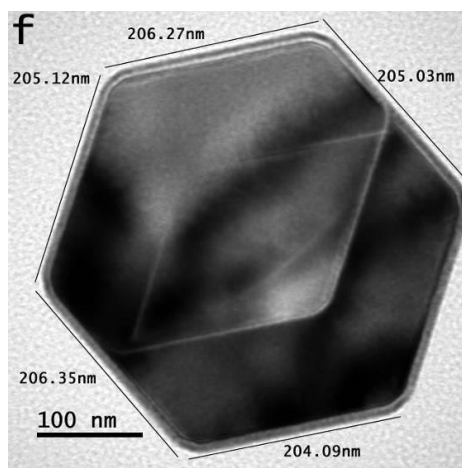
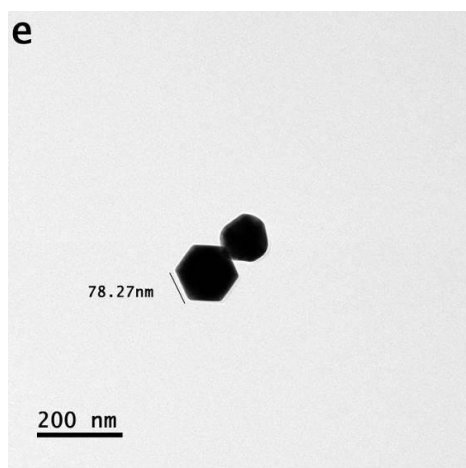
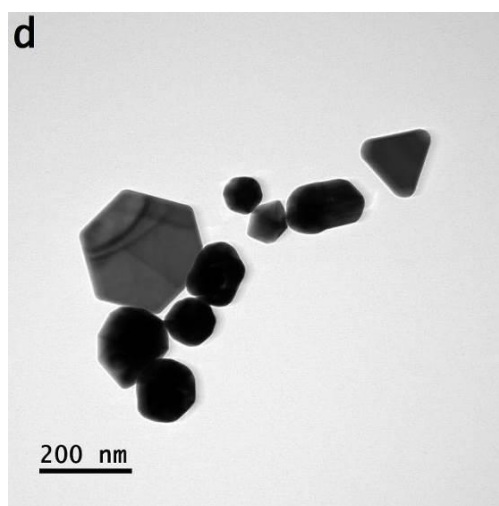
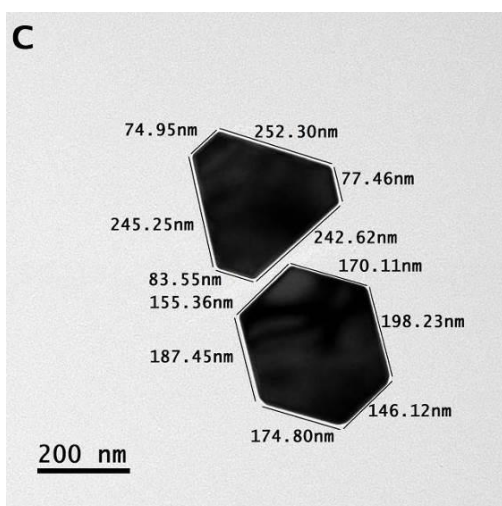
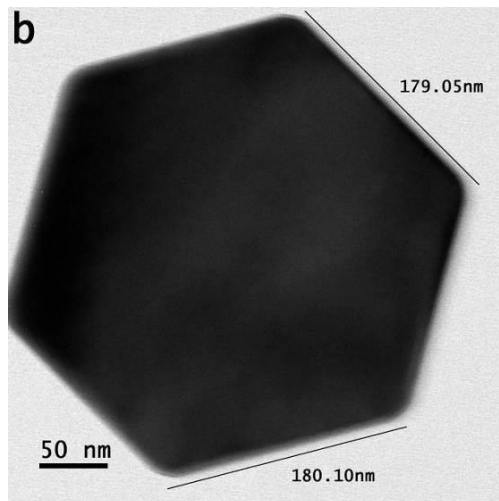
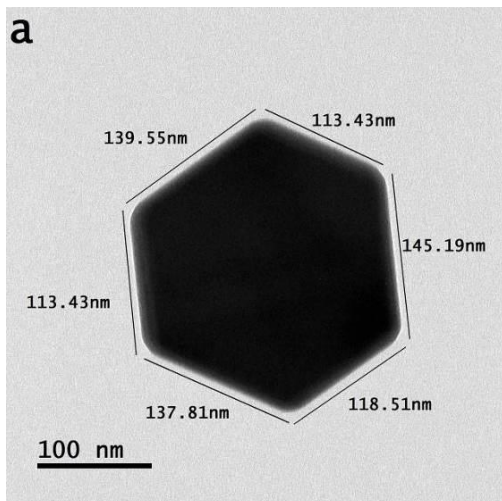


Figure S8: Bright field transmission microscope images of nanoparticles/particles showing both anisotropic and distorted shapes; precursor concentration 0.30 mM and argon flow rate 50 sccm



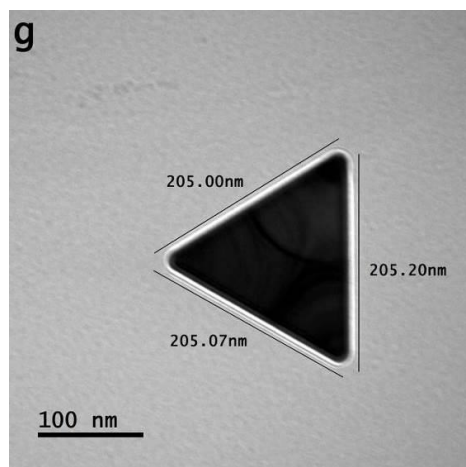


Figure S9: Bright field transmission microscope images of particles showing both geometric anisotropic shapes and distorted shapes; precursor concentration 0.60 mM and argon gas flow rate 50 sccm

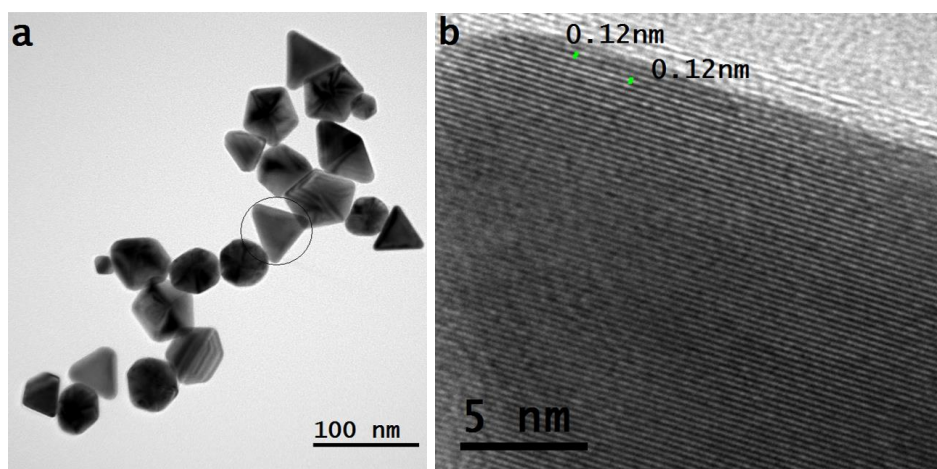


Figure S10: (a) Bright field transmission microscope image of nanoparticles showing both geometric anisotropic and distorted shapes at 0.10 mM and (b) magnified high-resolution transmission microscope image taken from the encircled triangle in 'a' shows equal width of structure of smooth element and inter-spacing distance; precursor concentration 0.10 mM and argon gas flow rate 50 sccm